



Published in final edited form as:

Reprod Toxicol. 2011 April ; 31(3): 280–289. doi:10.1016/j.reprotox.2010.10.002.

Neonatal exposure to genistein adversely impacts the ontogeny of hypothalamic kisspeptin signaling pathways and ovarian development in the peripubertal female rat

Sandra M Losa, Karina L Todd, Alana W Sullivan, Jinyan Cao, Jillian A Mickens, and Heather B Patisaul

North Carolina State University, Department of Biology, Raleigh, NC 27695

Summary Sentence

Neonatal genistein exposure at physiologically relevant levels advances vaginal opening, disrupts ovarian development and defeminizes the ontogeny of kisspeptin signaling pathways in the female rat hypothalamus.

Neonatal exposure to estrogenic endocrine disrupting compounds (EDCs) can advance pubertal onset and induce premature anestrous in female rats. It was recently discovered that hypothalamic kisspeptin (KISS) signaling pathways are sexually dimorphic and regulate both the timing of pubertal onset and estrous cyclicity. Thus we hypothesized that disrupted sex specific ontogeny of KISS signaling pathways might be a mechanism underlying these EDC effects. We first established the sex specific development of KISS gene expression, cell number and neural fiber density across peripuberty in the anteroventral periventricular nucleus (AVPV) and arcuate (ARC), hypothesizing that the sexually dimorphic aspects of KISS signaling would be most vulnerable to EDCs. We next exposed female rats to the phytoestrogen genistein (GEN, 1 or 10 mg/kg bw), estradiol benzoate (EB, 10 µg), or vehicle from post natal day (P) 0–3 via subcutaneous (sc) injection. Animals were sacrificed on either P21, 24, 28, or 33 (n = 5–14 per group at each age). Vaginal opening was significantly advanced by EB and the higher dose of GEN compared to control animals and was accompanied by lower numbers of KISS immunoreactive fibers in the AVPV and ARC. Ovarian morphology was also assessed in all age groups for the presence of multiple oocyte follicles (MOFs). The number of MOFs decreased over time in each group, and none were observed in control animals by P24. MOFs were still present, however, in the EB and 10 mg/kg GEN groups beyond P24 indicating a disruption in the timing of ovarian development.

Keywords

soy; kisspeptin; reproductive development; phytoestrogens; endocrine disruption; sexually dimorphic; brain; gonadotropin; estrogen; fertility; ovary

Corresponding author to whom all reprint requests should be addressed: Heather Patisaul, Assistant Professor, Department of Biology, North Carolina State University, Raleigh, NC 27695, (919) 513-7567, Heather_Patisaul@ncsu.edu.

Publisher's Disclaimer: This is a PDF file of an unedited manuscript that has been accepted for publication. As a service to our customers we are providing this early version of the manuscript. The manuscript will undergo copyediting, typesetting, and review of the resulting proof before it is published in its final citable form. Please note that during the production process errors may be discovered which could affect the content, and all legal disclaimers that apply to the journal pertain.

1. Introduction

The kisspeptin (KISS) family of proteins (previously called metastatins) derived from the *Kiss1* gene, is now recognized to play a critical role in signaling pubertal onset. The number of hypothalamic KISS neurons increases sharply around postnatal day (P) 30 in female rodents [1–2], an age which coincides with vaginal opening, a hallmark of pubertal onset in the rat. Chronic administration of KISS during the perinatal period accelerates pubertal onset in rats [1], emphasizing the potency of this peptide family on pubertal timing. KISS initiates puberty by stimulating the release of gonadotropin releasing hormone (GnRH) (reviewed in [3]). The KISS receptor (*Kiss1r*), a G-protein coupled receptor (previously identified as GPR 54), is constitutively expressed on GnRH neurons and stimulation of GnRH by KISS administration is sufficient to initiate pubertal development [4]. Humans (or mice) with a mutated form of *Kiss1r* fail to enter puberty and remain hypogonadal throughout life [5–6]. We have previously shown that neonatal exposure to GEN can advance age of vaginal opening in female rats [7]. Here, we sought to determine if this physiological indicator of puberty is accompanied by a premature increase of hypothalamic KISS levels.

Initially discovered in humans, similar systems have now been well characterized in other mammalian species including sheep, rodents, and non-human primates [8–10]. In the murine brain, there are two major populations of hypothalamic KISS neurons: one within and posterior to the anteroventral periventricular nucleus (AVPV) and one in the arcuate nucleus (ARC). It is currently unclear which is primarily responsible for initiating puberty. In sheep, monkeys, and humans, both populations of KISS neurons reside primarily in the ARC, but are functionally distinct. Thus, the rat is an appropriate model for studying the impact of endocrine disruption on each major population.

In adult rodents, the AVPV population is markedly sexually dimorphic, with females having substantially more *Kiss1* gene expression and immunoreactive KISS neurons and neuronal projections than males [2,11–14]. In contrast, the ARC population is not thought to be sexually dimorphic in adulthood because mRNA levels do not differ between the sexes [14]. The sex specific and region specific density of KISS neurons reflects the functional role of each population, and it is now widely hypothesized that the AVPV population regulates steroid positive feedback, while the ARC population regulates steroid negative feedback [3]. In the mouse AVPV, a sex difference in neuronal number is present as early as P10, with hypothalamic concentrations increasing steadily until P25 and then doubling between P25 and P30, a period which precedes the typical age at vaginal opening by a few days [2,15]. In contrast, the ontogeny of the ARC population has not yet been documented in detail. One goal of the present study was to address this crucial knowledge gap by quantifying KISS cell number, gene expression and fiber density across peripuberty. The need to elucidate the sex specific ontogeny of KISS signaling pathways in the ARC is enhanced by the recent hypothesis put forth by Kauffman and colleagues that KISS production by the ARC, rather than the AVPV, may be more essential for regulating pubertal timing [16]. Moreover, we hypothesized that the sexually dimorphic aspects of KISS signaling pathways would be most vulnerable to endocrine disruption because their organization is influenced by neonatal steroid hormones.

The neonatal critical period in rats is well appreciated to be a crucial hormone-sensitive window during which the hypothalamus undergoes sexual differentiation [17] and corresponds approximately to a similar window of sexual differentiation occurring in the human embryo during the third trimester [18]. Navarro and colleagues have reported that neonatal exposure to EB reduces *Kiss1* expression in the prepubertal rat brain (both sexes), but did not pinpoint where in the hypothalamus this takes place [19]. Thus the AVPV, the ARC, or both could be affected. We recently found that neonatal exposure to EB reduces the

density of KISS immunoreactivity (-ir) in the adult AVPV and ARC of the female rat [11], but did not look during peripuberty. Similarly, we found that neonatal exposure to GEN (10 mg/kg) also results in abrogated KISS-ir in the adult female AVPV, but not the ARC [7]. Changes in adult KISS-ir levels were accompanied by accelerated age at vaginal opening and premature anestrous suggesting that disrupted organization of KISS signaling pathways may be a mechanism underlying both effects. To explore this possibility, in the current study we examined the impact of neonatal EB or GEN exposure (at two doses) on KISS-ir levels in the AVPV and ARC from postnatal days 21 through 33 with the hypothesis that GEN exposure may accelerate the peripubertal rise in AVPV KISS-ir levels thereby advancing puberty.

There is growing evidence that perinatal exposure to doses of GEN considered relevant to human exposure levels impact the organization and development of the rodent female reproductive system, which then results in compromised fertility [20–21]. GEN is an isoflavone phytoestrogen found in soy and other legumes, and has been extensively studied for both its beneficial and endocrine disrupting properties [22–26]. Concern regarding the human health impacts of soy isoflavones like GEN has increased recently because rates of soy consumption in the West are rapidly growing (reviewed in [27]). Most notably, soy-based infant formulas constitute as much as a third of the infant formula market in the US. Infants maintained on these formulas consume as much as 6–9 mg/kg of isoflavone phytoestrogens per day which is 6–11 fold higher than a typical adult exposure [28]. Infants can also be exposed to GEN in utero through placental transfer or after birth via lactation [29–30]. The upper dose used for this study (10 mg/kg body weight) is approximately equivalent to the total amount of isoflavone phytoestrogens found in soy infant formulas, and the low dose (1 mg/kg body weight) was selected to model in utero exposure levels. Doses were given by injection, a route that obviously does not model human intake, but ensures consistent exposure between individuals and controls for interspecies differences in metabolism. Importantly, it has previously been shown that sc injection of 50 mg/kg, a dose 5-fold higher than the dose used for the present study, produces serum GEN levels within in the human range [31].

In addition to the brain, neonatal exposure to GEN has also been found to impact the development of the murine ovary. Jefferson and colleagues have shown that multiple oocyte follicles (MOFs) can be observed in the P19 mouse ovary following neonatal exposure to GEN either orally or by injection [32–33]. It is not clear if these MOFs are also induced by neonatal GEN exposure in the rat, or if they persist beyond pubertal onset. Interestingly, KISS and its receptor have been identified in the ovary [34–35], indicating that it may be an additional site vulnerable to disruption by GEN and other EDCs. Therefore, in the present study, we also determined whether neonatal GEN exposure results in MOFs in the rat ovary and if the number changes as pubertal onset approaches.

2. Materials and Methods

2.1 Animals and Conditions

Animal care and maintenance were conducted in accordance with the applicable portions of the Animal Welfare Act and the U.S. Department of Health and Human Services' "Guide for the Care and Use of Laboratory Animals" and approved by the North Carolina State University (NCSU) Institutional Animal Care and Use Committee. All litters (Long Evans or Wistar strain, originally obtained from) were born to animals bred in house or from time pregnant dams (Charles River, NC). The litters were culled to 12 on the day of birth (day of birth defined as postnatal day zero (P0)), ensuring that every litter had at least 3 males to minimize maternal rejection of the litter. All dams were individually housed and maintained on a 12 hour light cycle (lights on from 7:00 to 19:00) at 23°C and 50% average relative

humidity at the Biological Resource Facility at NCSU and maintained on a semi-purified, phytoestrogen-free diet ad libitum for the duration of the study (AIN-93G, Test Diet, Richmond, IN).

2.2 Experiment 1: Establish the sex specific ontology of KISS-ir in the male and female rat AVPV and ARC

To date, the density of AVPV KISS neurons has most frequently been quantified by immunolabeling the neurons and then counting the region-specific number of KISS immunoreactive (-ir) cell bodies [2,15]. Most of this work has been done in mice. Unfortunately, in the rat, AVPV KISS-ir cell bodies are not easily visualized, (point of discussion, 1st World Conference on Kisspeptin Signaling in the Brain, October 2008, Cordoba, Spain). In addition, within the ARC of both mice and rats, cell bodies are difficult to discern among the dense fiber labeling, especially in older animals [2,7,11,15]. As an alternative, we have previously demonstrated that KISS-ir is localized to extended lengths of fibers throughout the AVPV and ARC and have developed a method for quantifying these fibers, described in detail elsewhere [7,11]. To ensure that this method is a reasonable approach for looking at the impact of GEN on the sex specific ontology of KISS signaling pathways, we first compared the density of AVPV KISS-ir fibers in peripubertal male and female Wistar rats to AVPV Kiss1 mRNA levels across the same time period. In the ARC, because KISS-ir cell bodies can sometimes be visualized with confocal microscopy, we compared the difference between Kiss1 mRNA levels, KISS-ir fibers, and KISS-ir cell bodies.

2.2.1 In situ hybridization for Kiss1 mRNA—For quantification of AVPV and ARC Kiss1 mRNA, Wistar pups aged P10, 20 and 30 (n = 5 per sex per age) were pulled from our existing colony (from three different litters to ensure genetic heterogeneity) and sacrificed by rapid decapitation. The brains were then removed and flash frozen on crushed dry ice and stored at -80°C. The frozen brains were then cut into 20 µm coronal sections using a cryostat, slide mounted (Super Frost Plus slides, Fisher Scientific, Pittsburgh, PA) and stored at -80°C until processing for radiochemical in situ hybridization (ISH) using a standard protocol similar to what we and others have employed previously [13,36–38].

The cDNA transcriptional template generated to probe Kiss1 mRNA was a 318-bp cDNA insert (Genbank Accession number NM_181692.1) prepared by using reverse transcription–polymerase chain reaction (RT-PCR) with a forward primer of 5'-TCTCCTCTGTGTGGCCTCTT-3' and a reverse primer of 5'-AGGCCAAAGGAGTTCCAGTT-3'. This fragment was cloned into PCRII-TOPO vector, which was used to transform One Shot[®] TOP10 chemically competent E.Coli cells according to the user manual (Invitrogen, Carlsbad, CA). The plasmid was isolated from select colonies and sequenced to verify sequence, size and orientation (GENEWIZ Inc., South Plainfield, NJ). Antisense and sense Kiss1 probes were transcribed from linearized plasmid with T7 or SP6 respectively. Radiolabeled probes were synthesized by spinning down 15 µl of NEG ³⁵S-labeled UTP (PerkinElmer, Boston, MA) in a vacuum centrifuge and adding the following ingredients in a final volume of 10 µl: 2.0 µl 5X transcription buffer, 1.0 µl 100 mM DTT, 1.5 µl 3.3 mM ATP, GTP, CTP mix (Promega, Madison, WI), nuclease-free water and 1.0 µg linearized template. The reaction progressed at 37°C for 90 minutes with additional enzyme added at 30 minutes. Residual DNA was digested by adding RQ1 RNase-Free DNase (Promega, Madison, WI) in the final 30 minutes of the reaction. Finally, the cRNA probe was purified by Qiaquick Nucleotide Remove Kit (Qiagen, Valencia, CA) according the user manual.

Slides containing the AVPV and ARC were prehybridized as described previously [37]. Radiolabeled antisense Kiss1 riboprobes were denatured, dissolved in hybridization solution along with tRNA and 25 μ l (1×10^6 cpm) and applied to each slide. As a negative control, a subset of slides was incubated with radiolabeled sense probe. Slides were then covered with glass coverslips, and incubated overnight at 50°C in humid chambers. The next morning the slides were washed as described previously [37] and dehydrated in ascending concentrations of ethanol.

2.2.2 Generation and quantification of Kiss1 autoradiograms—Following ISH, slides were exposed to Kodak Biomax MR X-ray film (Eastman Kodak, Rochester, NY, USA) for 11 days (AVPV) or 24 days (ARC) then developed using an automatic processor (Konica Corporation, Tokyo, Japan). ¹⁴C-Labeled autoradiographic standards (Amersham Pharmacia Biotech) were included in the cassettes for quantification. X-ray film images were viewed using a monochrome QICAM 1394 12-bit camera (QImaging, Surrey, British Columbia, Canada) mounted above a light-box (Northern Lights; Berthold Australia). Relative levels of Kiss1 mRNA in the AVPV and ARC were assessed by optical density from the film autoradiograms using the digital densitometry application of the MCID Core Image software program (InterFocus Imaging Ltd, Cambridge, England) and following procedures similar to what we and others have described previously [36,39–40]. For each region of interest (AVPV or ARC), a sampling template encompassing the region of interest was created and used for all sections to standardize the area examined. Brain regions and background levels were measured unilaterally from anatomically matched sections. For each animal, six measurements per region of interest were obtained (two each from the rostral, medial and caudal regions) along with an unlabeled background area at each point. The six values obtained for each animal were then averaged to obtain a representative measurement for that animal. Average background levels were then subtracted to obtain a final value. Optical densities were converted to nCi/g tissue equivalents using autoradiographic ¹⁴C microscales (Amersham Life Sciences, Arlington Heights, IL, USA). In the ARC, insufficient tissue of adequate quality was available on P10, so only the results from the P20 and P30 animals were statistically analyzed.

2.2.3 Immunohistochemistry—For the immunohistochemical (IHC) labeling of KISS in the AVPV and ARC, siblings of the Wistar pups used for the ISH were pulled from our existing colony on Ps 5, 10, 20 and 30 (n = 5 per sex per age). P5 animals were sacrificed by rapid decapitation and the brains were immersion fixed in cold 4% paraformaldehyde for 24 hours, postfixed for 24 hours in 4% paraformaldehyde containing 20% sucrose, then cryoprotected overnight at 4°C in potassium phosphate buffer (KPBS) containing 20% sucrose. P10 animals were sacrificed by transcardial perfusion with 4% paraformaldehyde, then, to enhance fixation, postfixed overnight at 4°C in 4% paraformaldehyde, postfixed for an additional 24 hours in 4% paraformaldehyde containing 20% sucrose, then cryoprotected for 24 hours. All other animals were sacrificed by transcardial perfusion with 4% paraformaldehyde, postfixed overnight in 4% paraformaldehyde containing 20% sucrose, and then cryoprotected for 24 hours. All brains were then frozen on crushed dry ice and stored at –80°C until IHC processing (see below). Prior work has shown that AVPV KISS levels at P5 are undetectable [2,15], thus we did not quantify AVPV KISS-ir levels in this age group. In addition, insufficient tissue of adequate quality was available for the P20 animals. Thus, for the AVPV, only P10 and 30 animals were ultimately examined. For the ARC, all age groups and time points were examined.

Perfused brains were sliced into 35 μ m coronal sections using a freezing sliding microtome, divided into two series of free-floating alternating sections and stored in antifreeze (20% glycerol, 30% ethylene glycol in KPBS) at –20°C [41]. One set of hypothalamic sections containing the organum vasculosum of the lamina terminalis (OVLT) through the caudal

border of the AVPV were immunolabeled for KISS using IHC techniques described in detail elsewhere [11]. KISS was detected using a rabbit anti-human kisspeptin antibody raised against amino acids 43–52 (at 1:8000) generously gifted by Dr. Alain Caraty, University Tours/Haras Nationaux, Nouzilly, France [42]. After a 72 hour incubation in the primary antibody at 4°C, the sections were placed in Alexa-Fluor goat anti-rabbit 555 secondary antibodies for 90 minutes and rinsed. Sections were then mounted onto slides (Superfrost Plus, Fisher, Pittsburgh, PA) and cover-slipped using a glycerol based mountant (50% glycerol in 4M sodium bicarbonate). A second set of brain sections comprising the rostral to caudal borders of the ARC were immunolabeled for KISS using the same immunohistochemical procedures.

2.2.4 Quantification of KISS-ir fiber density in the AVPV and ARC—Because AVPV KISS neurons are not easily visualized, we have developed a method for quantifying KISS-ir localized within extended lengths of fibers throughout the AVPV and ARC [7,11]. This method does not quantify all fibers, thus the values are meant to be a representative sample of KISS-ir within each region. For Experiment 1, three anatomically matched AVPV sections per animal (n = 5 per sex, aged P10 and 30), comprising the caudal, medial and rostral regions, were quantified. Tissue selection was accomplished with the assistance of a rat brain atlas[43]. In the ARC, three sections per animal (n = 5 per sex, aged P5, 10, 20 and 30) encompassing the caudal, medial and rostral regions, were also selected and quantified.

The AVPV and ARC tissue was visualized on a Leica TCS SPE confocal microscope using a 40X corrective objective lens. For every scan a set of serial image planes (z-step distance = 1µm) was collected through the entire slice of tissue. Image stacks were analyzed using the Image J software package (National Institute of Health (NIH), Bethesda, MD), described in detail elsewhere [7,11]. To control for variation in tissue thickness for each animal the confocal stacks were reduced to substacks of 17 consecutive image planes (for each region). Individual images in the substacks were first binarized and depixelated to minimize the inclusion of background fluorescence. Next, the fibers were skeletonized to a thickness of 1 pixel to control for variation in fiber thickness and brightness. Finally, the resulting pixels in each plane were quantified using the Image J Voxel Counter plug-in (NIH). The number of voxels within the stack was then averaged to give a representative density of KISS-ir voxels within the region of interest for each animal. This process was completed independently by two people, both blind to the exposure groups. The values obtained by each were then averaged together to create the data set used for the analysis [7,11].

2.2.5 Quantification of KISS-ir cell bodies in the ARC—Because an appreciable sex difference in KISS-ir fiber density was only observed on P20 and 30, KISS-ir cell bodies were only counted at these two time points. The same sections used to quantify fiber density were visualized on the Leica TCS SPE confocal using a 10x corrective objective lens with a 1.5x digital zoom. For each section, stacks of serial image planes (z-step distance = 2.5 µm) were collected through the entire tissue thickness. KISS-ir cells were then counted by hand by an observed blind to the treatment groups and summed across all three sections per animal to obtain a final total.

2.3 Experiment 2: Neonatal exposure to vehicle, EB or GEN

Litters were generated from our existing Long Evans rat colony (n = 30) or time pregnant rats (n = 18; Charles River) and maintained on a soy-free diet. Wistars were not used because the colony was not large enough at the time. Starting on the day of birth, the pups were subcutaneously (sc) injected with the vehicle (0.05ml sesame oil, Sigma, Saint Louis, MO), estradiol benzoate (EB, 10 µg, Sigma), 1mg/kg body weight (bw) GEN (1GEN, Indofine Chemical Company, Hillsborough, NJ), or 10mg/kg bw GEN (10GEN). Injections

were administered every 24 hours for 4 days (P0-3). It is well established that sexual differentiation of KISS feedback circuit occurs during this neonatal critical period in rodents and can be altered by hormone exposure [7,12]. This neonatal window in rats can be approximately equated with the sexual differentiation occurring in the human embryo during the late second and third trimesters [18]. EB was used as a positive control since it has previously been established that neonatal exposure at this concentration defeminizes the female hypothalamus [7]. All compounds were dissolved in 100% ethanol (EtOH, Pharmaco), and then sesame oil at a ratio of 10% EtOH and 90% oil as our lab has done previously [7]. Although we recognize and acknowledge that injection does not model a typical human oral exposure, because this was primarily a mechanistic study, injection was used in this instance to ensure that all of the pups received the exact same dose and that individual differences in metabolism did not impact the results. The pharmacokinetics of oral versus injected GEN has been published previously [31–32].

On P21, all animals were weaned into same-sex littermate groups of up to 4 and ear punched for identification. The females were maintained on the same light cycle, housed in the same room as the dams and maintained on the phytoestrogen-free diet. The male pups were removed from the room at weaning and not used for this study. At the time of perfusion, the animals were checked for vaginal opening, a hallmark of pubertal onset in the rat.

2.3.1 Brain and ovarian tissue collection—The female pups were transcardially perfused between 10am and 12pm with 4% paraformaldehyde on either P21, 24, 28 or 33. To control for potential litter effects, no more than two pups per litter were used in each age group. Therefore, within each age group, pups came from a minimum of three mothers. After perfusion the brains were removed, post-fixed and cryoprotected as described in Experiment 1, for P20 and P30 animals. In addition to the brains, the ovaries were also removed at sacrifice and post-fixed in 4% paraformaldehyde for 24 hours on a shaker at 4°C, then switched to 70% EtOH and stored at 4°C for another 48 hours and transferred to fresh 70% EtOH and stored at 4°C until sectioning.

2.3.2 Immunohistochemistry and Quantification of KISS-ir fiber density in the AVPV and ARC—For Experiment 2, because the sheer volume of tissue was considerably high, only a single, midlevel AVPV section (corresponding to Figure 33 in the 2004 edition of the Paxinos and Watson Rat Brain Atlas), and a single midlevel ARC section (corresponding to Figure 59) were selected for analysis. Data from Experiment 1 indicated that this would be sufficient to detect significant sex differences in KISS-ir fiber density within each region. Confocal image stacks were then collected and analyzed as described in Experiment 1.

2.3.3. Processing of Ovarian Tissue—The ovaries were sent to The Hamner Institute (Research Triangle Park, NC) for paraffin embedding, sectioning and histological processing, then returned to NC State for analysis. Both ovaries from each animal were cut into 5 µm sections, and slide mounted (Superfrost Plus, Fisher). Two sections 100 µm apart for each ovary were stained with a progressive H&E stain to visualize the follicles. The number of multiple oocyte follicles (MOF) present in each ovary was then counted by hand using a Leica 5000DM microscopy an observer blind to the treatment groups and summed for each animal. Because of technical issues, ovarian tissue was not available from all of the P28 or P33 animals. Thus the observations are presented here, but the resulting data was not statistically analyzed for group differences.

2.4 Statistical Analysis

For Experiment 1, a two-way ANOVA with age and sex was first performed to identify group differences. Significant findings were followed up by one-way ANOVA and Fisher's Least Significant Difference (LSD) post hoc tests to identify statistically significant sex differences in Kiss1 mRNA levels, ARC KISS-ir cell bodies and KISS-ir fiber density. For Experiment 2, there were four different exposure groups: OIL, 1GEN (1mg/kg), 10GEN (10mg/kg) and EB. Additionally there were four time points (ages) in each exposure group: P21, 24, 28 and 33. KISS fiber density was first compared by two-way ANOVA with age and exposure as factors. This was followed by two one-way ANOVAs, one for exposure and one for age, followed by LSD post hoc tests when appropriate. In all cases significance level was set at $p < 0.05$ (SYSTAT 13.0).

3. Results

3.1 Experiment 1: Peripubertal KISS-ir levels are sex specific

As expected, there was a significant effect of both age ($F = 9.675, p \leq 0.007$) and sex ($F = 25.614, p \leq 0.001$) on the density of AVPV KISS-ir neuronal fibers. Levels increased in both males and females between P10 and P30 (Fig. 1A) and a trend for a statistically significant sex difference emerged by P30 ($p = 0.08$). Females had twice as many KISS-ir fibers as males on P30. The ontogeny of Kiss1 mRNA levels had a similar pattern (Fig. 1B and C) validating the use of fiber density as a reasonable indicator of the sexual dimorphic ontogeny of the kisspeptin system in the AVPV. Two-way ANOVA revealed a significant effect of sex ($F = 14.8, p \leq 0.001$) but only a trend for an effect of age ($F = 2.04, p \leq 0.15$). Sex differences in expression were statistically significant on P10 ($p \leq 0.03$) and P30 ($p \leq 0.05$).

The sexually dimorphic ontogeny of KISS-ir was even more pronounced in the ARC (Fig 1D-F). Two-way ANOVA revealed a significant effect of age ($F = 19.121, p \leq 0.001$) and sex ($F = 47.651, p \leq 0.001$) on the density of ARC KISS-ir neuronal fibers. Levels were relatively low in both sexes until P20, at which point female levels escalated to approximately five times higher than male levels ($p \leq 0.004$). This sex difference persisted to P30 ($p \leq 0.01$). A concomitant sex difference in mRNA levels was not observed, however (Fig 1E). Two-way ANOVA identified a significant effect of age ($F = 21.695, p \leq 0.001$), with levels declining in both sexes over time, but not an effect of sex. Post hoc analysis revealed a trend for a sex difference on P20 ($p = 0.07$) but not P30. Similarly, as described previously for both the mouse and the rat [2,7,11,15], KISS-ir cell bodies in the ARC were difficult to visualize due to heavy fiber labeling, but from what could be discerned using the confocal microscope, no significant differences in cell number at either P20 ($p = 0.712$) or P30 ($p = 0.618$) were observed. Collectively these data indicate that fiber density is a more robust and easily quantifiable measure of KISS immunolabeling in this region. Moreover, the pronounced sex difference indicates that this aspect of KISS signaling pathways in the ARC may be most sensitive to endocrine disruption.

3.2 Experiment 2: Neonatal exposure to GEN decreased KISS fiber density in the peripubertal AVPV of female rats

Two-way ANOVA revealed a significant effect of exposure and age on KISS-ir fiber density in the AVPV of female LE rats ($F(3,119) = 18.149, p \leq 0.001, F(3,119) = 5.544, p \leq 0.001$ respectively). As seen in the Wistar rats used for Experiment 1, AVPV KISS-ir levels increased over time in the vehicle exposed control females (Fig. 2). An appreciable increase was not observed, however, in the EB or 10GEN exposure groups, a pattern which is more typical of males, based on observations made in Experiment 1. One-way ANOVA was used to test for group differences at each age. A significant effect of exposure was observed on

P21 ($F(3, 23) = 5.041, p \leq 0.008$), P24 ($F(3,33) = 10.780, p \leq 0.001$), P28 ($F(3,33) = 7.744, p \leq 0.001$) and P33 ($F(3,30) = 2.901, p \leq 0.05$). On P21, KISS-ir levels were significantly lower in the EB exposed females compared to the vehicle exposed controls ($p \leq 0.05$). By P24, all three exposure groups (EB, 10GEN and 1GEN) had significantly lower KISS-ir fiber density compared to control females ($p \leq 0.003$ in all cases). On P28, only EB and 10GEN exposed females had significantly fewer KISS-ir fibers compared to the controls ($p \leq 0.003$ in each case). On P33, KISS-ir levels were only significantly lower in EB exposed females ($p \leq 0.007$), while a nonsignificant trend for lower levels was observed in the 10GEN group ($p = 0.1$).

3.3 Experiment 2: KISS fiber density in the ARC was minimally affected by neonatal exposure to GEN

Two-way ANOVA indicated a significant effect of exposure and age on KISS-ir fiber density in the ARC ($F(3,106) = 83.567, p \leq 0.001$, $F(3,106) = 7.330, p \leq 0.001$ respectively), as well as a significant interaction of exposure and day ($F(9,106) = 3.365, p \leq 0.001$). As observed in the Wistar females used for Experiment 1, KISS-ir levels increased over time in the vehicle exposed control animals (Fig. 2). KISS-ir fiber density in the EB exposed animals, however, remained relatively flat and thus more typical of the male pattern observed in Experiment 1. One-way ANOVA was used to test for group differences at each age. A significant effect of exposure was observed on P21 ($F(3,21) = 20.217, p \leq 0.001$), P24, $F(3,31) = 34.124, p \leq 0.001$), P28 ($F(3,27) = 24.529, p \leq 0.001$) and P33 ($F(3,27) = 21.985, p \leq 0.001$). EB exposed animals had significantly fewer KISS-ir fibers compared to vehicle exposed animals at all ages ($p \leq 0.001$). On P21, the 1GEN and 10GEN females had a significantly lower KISS-ir compared to controls ($p \leq 0.04$ and $p \leq 0.014$ respectively). On P24, 28 and 33, although levels consistently remained lower in the 10GEN animals compared to controls, the difference was no longer statistically significant. In contrast, levels in the 1GEN animals oscillated over time and were statistically lower than control animals on P33 ($p \leq 0.032$).

3.4 Experiment 2: Neonatal GEN exposure advanced day of vaginal opening

Vaginal opening was assessed on the day of perfusion (Table 1). EB exposed animals experienced vaginal opening first, (25% of P21 females and 100% of P24 females) followed by the 10GEN and 1GEN exposed animals (none of P24 females, but 100% of P28 females), and lastly the vehicle exposed control animals (none of P28 females, but 100% of P33 females).

3.5 Experiment 2: Ovarian development is affected by neonatal GEN exposure

Because ovarian tissue was not available from P28 10GEN, P33 10GEN, or P33 OIL exposed animals, this data was not statistically analyzed for group differences and is presented for descriptive purposes only (Fig. 3). On P21, 60% ($n = 5$) of the control animals had MOFs, but no animal had more than 1. At the same time point, 100% ($n = 5$) of the 10GEN exposed animals had MOFs, ranging in number from 1 to 8 per animal. On P24 ($n = 3$), none of the control animals had MOFs, while MOFs were still counted in 17% of the 10GEN exposed animals ($n = 6$).

4. Discussion

Our results from Experiment 1 recapitulate and support prior reports that the ontogeny of AVPV KISS signaling pathways in early development is sexually dimorphic. We also show, for the first time, the ontogeny of KISS in the ARC across development, and reveal that only KISS-ir fiber density is sexually dimorphic in this region during peripuberty. Experiment 2 results demonstrate that this sex specific organization is vulnerable to endocrine disruption

in females, an observation that may indicate a potential mechanism for disruption of pubertal timing and the premature onset of anovulation. Females neonatally exposed to EB had perinatal KISS-ir levels that were male-like at all ages examined. This observation demonstrates that exposure to estrogen during this developmental critical window results in persistent abrogation of KISS-ir, a pattern suggestive of defeminization. The 10GEN animals also had decreased levels of AVPV KISS-ir compared to controls, the magnitude of which was not as pronounced as in the EB females. In contrast, the effects of neonatal exposure to 1GEN were more ambiguous but similar to control animals. These data do not support our initial hypothesis that the perinatal rise in KISS-ir levels in female rats would be accelerated by neonatal exposure to GEN.

The sex specific increase in AVPV KISS-ir fiber density in the peripubertal rat reported here is consistent with findings previously observed by other labs in mice [2,15]. In the female mouse AVPV, the number of KISS neurons and the density of Kiss1 mRNA expression increases between P10 and P31, with few to no neurons present on P10 [2,16]. A similar increase in AVPV KISS neuron number has also been observed in age matched males, however, the overall magnitude of the increase is lower in males and occurs a few days later than in females [2]. Here we report, for the first time, a similar developmental pattern of sexually dimorphic KISS-ir fiber density in the rat AVPV, an observation which is technically useful because KISS cell bodies are notoriously difficult to immunolabel in the rat. A different picture, however, emerged in the ARC. We found a pronounced sex difference in KISS-ir fiber density but no difference in the number of KISS neurons or Kiss1 mRNA. These neurons are difficult to visualize, so technical issues may be a factor in the discrepancy but the observations are consistent with a prior study which established that Kiss1 mRNA levels do not differ by sex in the adult ARC [12]. Previous studies have not shown the ontogeny of ARC KISS-ir fiber density across development [44], therefore results obtained from Experiment 1 fill this important knowledge gap. Parallel work in our laboratory has revealed that a sex difference in Kiss1 mRNA levels exists prior to P20. This difference is most pronounced in neonatal animals and declines as P20 approaches (publication pending, Cao and Patisaul), a finding in good agreement with what was observed in the P20 animals of the present study.

Collectively, these studies by us and others indicate that, although females have a denser network of KISS-ir neuronal fibers within the ARC compared to males, this difference is not reflected in Kiss1 mRNA expression or cell number. These observations strongly support the hypothesis that the sex difference in ARC KISS-ir fiber density results from a higher number of projections arising from the AVPV population proceeding caudally to the pituitary by way of the ARC and median eminence, because females have significantly more KISS neurons in the AVPV than males. Track tracing studies would be needed to verify this postulate.

The observed sex and regional differences in KISS-ir across peripuberty are functionally relevant because the two populations of KISS neurons are hypothesized to regulate different aspects of the hypothalamic-pituitary-gonadal (HPG) axis. It is now widely accepted that the AVPV population mediates the preovulatory release of gonadotropins through steroid positive feedback, and has been shown to be most active around the time of ovulation [3,12,45–47]. In contrast, the ARC population is thought to be more critical for steroid negative feedback in both sexes. It has previously been reported that neonatal androgen exposure can result in decreased Kiss1 mRNA expression in the AVPV of female rats, thereby resulting in more male-typical levels [12]. Here we have shown a similar effect of neonatal EB exposure in female rats on AVPV KISS-ir, suggesting that the male-typical levels observed in the previous study resulted from the action of estrogens aromatized from

the administered androgens. It remains unclear if or how the lower levels of ARC KISS-ir observed in the EB exposed female animals might impact steroid negative feedback.

We have further shown that neonatal exposure of female rats to the phytoestrogen GEN can also result in more male-like ontogeny of AVPV KISS-ir. Although this observation does not support our initial hypothesis that the peripubertal elevation in KISS-ir levels would be accelerated in GEN exposed animals, it is instead consistent with prior data from our lab indicating that neonatal GEN exposure can defeminize the hypothalamus. For example, we have already established that this significant abrogation of AVPV KISS-ir in 10GEN animals persists into adulthood, demonstrating that the effect is permanent [7]. Moreover, we have found that reduced AVPV KISS-ir is accompanied by premature anestrus and impaired steroid feedback on GnRH neurons [7], observations which are consistent with the hypothesis that disruption of AVPV KISS signaling pathways can abrogate or eliminate the capacity for steroid positive feedback leading to reproductive disruption in females. By contrast, the impact of 10GEN exposure on KISS-ir in the peripubertal female ARC was less pronounced. Levels remained lower over time compared to control animals but not significantly so, and were markedly higher than in the EB exposed females. We have previously reported a similarly small but not statistically significant difference in the adult female ARC [7], indicating that this marginal reduction persists into adulthood. This developmental pattern is distinct from what we observed in the EB exposed females. In that group, KISS-ir levels remained low across peripuberty and we have previously found that they remain low in adulthood [7]. Collectively, our results indicate that the sexual differentiation of the AVPV KISS population begins prior to puberty and that the peripubertal window is a time of significant sex specific organization. Moreover, our findings emphasize the adverse lifelong consequences of early life exposure to estrogenic endocrine disruptors on female reproductive neuroendocrinology.

The magnitude and region specific impact of EB and GEN on KISS-ir in female rats might be related to the different relative binding affinities these compounds have for the nuclear estrogen receptor (ER) subtypes α and β . The type and density of ER subtypes found in the AVPV and the ARC may also be a factor. In the adult AVPV, KISS neurons are co-localized with both ER α and ER β , while in the ARC, KISS neurons are most frequently found to co-express ER α [45]. In vitro studies have revealed that GEN has a higher relative binding affinity for ER β than ER α [48–49]. This higher binding affinity for ER β combined with the region specific distribution of ER β in KISS neurons might explain why the impact of GEN in the AVPV is more pronounced and persistent than in the ARC. It is also possible that GEN is acting via multiple mechanisms to impact KISS-ir. For example, GEN has long been recognized to be a potent tyrosine kinase inhibitor [50]. In addition, new estrogen receptors have now been identified such as GPER (formerly known as GPR30) and ERR3 (also called estrogen-related receptor gamma) [51–53] any of which might be responsive to GEN during neonatal life. Alternatively, disruption could have occurred elsewhere in the HPG axis, such as the ovary, resulting in improper signaling between each of the components and manifesting as male-like development in the hypothalamus.

Numerous prior studies indicate that neonatal exposure to isoflavones or estrogens during neonatal development can result in altered ovarian morphology in mice [32,54–56] and our observation that neonatal exposure to EB or the higher dose of GEN impacted ovarian organization in rats is consistent with that body of work. MOFs are common as the ovary matures and oocytes differentiate into primordial follicles, and thus are only typically observed early in the peripubertal period [57]. Our observation that MOFs were only present at very low numbers in control P21 females is indicative of normal development. In contrast, increased numbers of MOFs were observed at all ages in females neonatally exposed to EB. Similarly, we found increased numbers of MOFs through P24 in 10GEN females. Oral

exposure to GEN or the glycosylated form found in foods (genistin) in the neonatal window has previously been shown to result in significantly increased numbers of MOFs in P19 mice [32–33] but the authors did not look beyond that time point. Our results reveal that abnormally high numbers of MOFs persist through P24 but then drop. We have previously shown that in adults exposed to 10mg/kg GEN neonatally, the ovaries contain numerous cyst-like structures and few to no corpora lutea (indicative of anovulation) but no MOFs [7], thus the observation that the number of MOFs ultimately decreased was not completely unexpected.

Increased number of MOFs following GEN exposure could result from a direct effect of GEN on the ovary itself, or as a consequence of disrupted neuroendocrine signaling pathways in the brain. The former is more likely because prior work has shown that, in cultured ovaries, the oocyte nests present at birth properly separate and establish the primordial follicle pool, demonstrating that no signal from the brain is needed to complete neonatal ovarian maturation [55,58]. Moreover, GEN exposure has been shown to directly inhibit oocyte nest breakdown and primordial follicle assembly both *in vivo* [59] and *in vitro* [55], effects also induced by progesterone or estrogen exposure [55,60] suggesting that GEN and estrogen may have similar mechanisms of action. Programmed cell death of oocytes is a normal and critical part of ovarian maturation and occurs at the time of oocyte nest breakdown, suggesting that it is required for nests to break apart [58]. The observed delay in the reduction of MOFs in the 10GEN females is suggestive of delayed ovarian development, and the reduction in the number of MOFs in the older animals could indicate that these cells ultimately undergo programmed cell death leading to few [56] or no MOFs in adulthood [61].

Delayed ovarian maturation in the EB and 10GEN animals was accompanied by significantly lower AVPV KISS-ir, thus it is plausible that ovarian development could drive the pace of hypothalamic KISS pathway organization. In adult females, Kiss1 mRNA in the AVPV is up-regulated by endogenous estrogens released from the adult ovary [45–46]. Delayed ovarian development may result in lower circulating estrogen levels across peripuberty, and consequently a male-like pattern of KISS-ir development. Circulating estrogen levels were not assessed in the present study, but prior work has shown that circulating estradiol and progesterone levels in prepubertal mice neonatally exposed to 0.5, 5 or 50 mg/kg GEN on PND 19 or 5–6 weeks of age are no different from control animals [62–63]. Thus, it is unlikely that circulating steroid hormone levels were affected in the present study. We hypothesize that GEN impacted the hypothalamus directly thereby disrupting the ontogeny of KISS signaling pathways.

The combination of delayed ovarian development and abrogated hypothalamic KISS-ir levels in EB and 10GEN females are suggestive of delayed pubertal onset, yet both groups displayed advanced vaginal opening, an event long interpreted [64–65], and still commonly used [66] as a hallmark of pubertal onset in the rat. Vaginal opening by itself, however, may not always be a reliable indicator of pubertal onset. Therefore the data obtained here either support the concern that vaginal opening is not a reliable measure of pubertal onset, or suggest that the timing of vaginal opening and maturation of the HPG axis are controlled by two different mechanisms. While advanced vaginal opening following prepubertal EB or GEN exposure is consistent with prior reports by us and others [7,20,59,67–70], the disconnect between hypothalamic and ovarian maturation further supports the possibility that vaginal opening may not be reflective of the pace at which the neuroendocrine components of the HPG axis are maturing. Alternatively, the timing of vaginal opening might be associated with KISS-ir levels in the ARC. This hypothesis is supported by findings that central administration of KISS can restore delayed vaginal opening in undernourished rats [71]. In both sexes, the ARC population of KISS neurons is proposed to

generate the signal necessary for GnRH secretion suppression through steroid negative feedback [12–13]. More recently the ARC has also been proposed to play a role in the timing of pubertal onset [16]. Both the EB and 10GEN exposed females had significantly lower levels of ARC KiSS-1r on P21 compared to control animals. Lower levels persisted in both groups, although the difference was not statistically significant in the 10GEN animals beyond P21. It is possible that the lower levels observed in the EB and 10GEN animals on P21 are not sufficient to inhibit gonadotropin release, and consequently these animals go through vaginal opening early. As stated previously, we did not determine circulating hormone levels in these animals but that information would be needed to further explore this hypothesis.

Here, we have shown that the maturation rate and sex specific ontogeny of the female reproductive system can be adversely impacted by neonatal exposure to estrogenic endocrine disruptors. These observations are consistent with the emerging Fetal Basis of Adult Disease (FEBAD) hypothesis [72–73] which purports that exposure to toxicants in early life, while hormone sensitive systems are still forming, could result in disease states such as precocious puberty, infertility and premature anestrus later in life. The presence of EDCs, both natural and synthetic, is increasing in the environment resulting in nearly ubiquitous human exposure. Notably, the use of soy products, including soy infant formula and other soy-based products directed at children, is increasing in Western society (reviewed in [27]) resulting in increasing phytoestrogen consumption levels. Simultaneously, epidemiological data suggest that pubertal onset is advancing in human females [74–75], and other reproductive disorders such as unexplained infertility and breast cancer are also on the rise [76]. Our data support the hypothesis that increasing levels of exposure to estrogen-like compounds, such as genistein, are contributing to adverse reproductive health trends such as early puberty and suggest that GEN exposure during critical life stages could result in abnormal reproductive development in girls.

Acknowledgments

This work was supported by National Institute of Environmental Health Sciences grant R01 ES016001 to H.B.P. The authors thank Barbara (BJ) Welker and Linda Hester for their assistance with animal husbandry. We also appreciate Delores Williams at the Hamner Institute for embedding and processing the ovarian tissue with the assistance of Betsy Bermudez. We gratefully acknowledge Wendy Jefferson and Retha Newbold of NIEHS for their guidance regarding how to evaluate ovarian development and appreciate the advice and support of Heather Adewale for her critical reading of this manuscript. We also appreciate the support of Kelly McCaffrey for her assistance with the in situ hybridization assay.

References

1. Navarro VM, Castellano JM, Fernandez-Fernandez R, Barreiro ML, Roa J, Sanchez-Criado JE, et al. Developmental and hormonally regulated messenger ribonucleic acid expression of KiSS-1 and its putative receptor, GPR54, in rat hypothalamus and potent luteinizing hormone-releasing activity of KiSS-1 peptide. *Endocrinology*. 2004; 145:4565–74. [PubMed: 15242985]
2. Clarkson J, Herbison AE. Postnatal development of kisspeptin neurons in mouse hypothalamus; sexual dimorphism and projections to gonadotropin-releasing hormone neurons. *Endocrinology*. 2006; 147:5817–25. [PubMed: 16959837]
3. Oakley AE, Clifton DK, Steiner RA. Kisspeptin signaling in the brain. *Endocr Rev*. 2009; 30:713–43. [PubMed: 19770291]
4. Messenger S, Chatzidaki EE, Ma D, Hendrick AG, Zahn D, Dixon J, et al. Kisspeptin directly stimulates gonadotropin-releasing hormone release via G protein-coupled receptor 54. *Proceedings of the National Academy of Sciences of the United States of America*. 2005; 102:1761–6. [PubMed: 15665093]
5. de Roux N, Genin E, Carel JC, Matsuda F, Chaussain JL, Milgrom E. Hypogonadotropic hypogonadism due to loss of function of the KiSS1-derived peptide receptor GPR54. *Proceedings of*

- the National Academy of Sciences of the United States of America. 2003; 100:10972–6. [PubMed: 12944565]
6. Seminara SB, Messager S, Chatzidaki EE, Thresher RR, Acierno JS Jr, Shagoury JK, et al. The GPR54 gene as a regulator of puberty. *The New England journal of medicine*. 2003; 349:1614–27. [PubMed: 14573733]
 7. Bateman HL, Patisaul HB. Disrupted female reproductive physiology following neonatal exposure to phytoestrogens or estrogen specific ligands is associated with decreased GnRH activation and kisspeptin fiber density in the hypothalamus. *Neurotoxicology*. 2008
 8. Smith JT. Kisspeptin signalling in the brain: steroid regulation in the rodent and ewe. *Brain research reviews*. 2008; 57:288–98. [PubMed: 17509691]
 9. Shahab M, Mastronardi C, Seminara SB, Crowley WF, Ojeda SR, Plant TM. Increased hypothalamic GPR54 signaling: a potential mechanism for initiation of puberty in primates. *Proc Natl Acad Sci U S A*. 2005; 102:2129–34. [PubMed: 15684075]
 10. Pompolo S, Pereira A, Estrada KM, Clarke IJ. Colocalization of kisspeptin and gonadotropin-releasing hormone in the ovine brain. *Endocrinology*. 2006; 147:804–10. [PubMed: 16293663]
 11. Patisaul HB, Todd KL, Mickens JA, Adewale HB. Impact of neonatal exposure to the ERalpha agonist PPT, bisphenol-A or phytoestrogens on hypothalamic kisspeptin fiber density in male and female rats. *Neurotoxicology*. 2009; 30:350–7. [PubMed: 19442818]
 12. Kauffman AS, Gottsch ML, Roa J, Byquist AC, Crown A, Clifton DK, et al. Sexual differentiation of Kiss1 gene expression in the brain of the rat. *Endocrinology*. 2007; 148:1774–83. [PubMed: 17204549]
 13. Gottsch ML, Cunningham MJ, Smith JT, Popa SM, Acohido BV, Crowley WF, et al. A role for kisspeptins in the regulation of gonadotropin secretion in the mouse. *Endocrinology*. 2004; 145:4073–7. [PubMed: 15217982]
 14. Kauffman AS. Sexual differentiation and the Kiss1 system: hormonal and developmental considerations. *Peptides*. 2009; 30:83–93. [PubMed: 18644414]
 15. Clarkson J, Boon WC, Simpson ER, Herbison AE. Postnatal development of an estradiol-kisspeptin positive feedback mechanism implicated in puberty onset. *Endocrinology*. 2009
 16. Kauffman AS, Navarro VM, Kim J, Clifton D, Steiner RA. Sex Differences in the Regulation of Kiss1/NKB Neurons in Juvenile Mice: Implications for the Timing of Puberty. *Am J Physiol Endocrinol Metab*. 2009
 17. Simerly RB. Wired for reproduction: organization and development of sexually dimorphic circuits in the mammalian forebrain. *Annu Rev Neurosci*. 2002; 25:507–36. [PubMed: 12052919]
 18. Grumbach MM. The neuroendocrinology of human puberty revisited. *Horm Res*. 2002; 57 (Suppl 2):2–14. [PubMed: 12065920]
 19. Navarro VM, Sanchez-Garrido MA, Castellano JM, Roa J, Garcia-Galiano D, Pineda R, et al. Persistent Impairment of Hypothalamic KiSS-1 System Following Exposures to Estrogenic Compounds at Critical Periods of Brain Sex Differentiation. *Endocrinology*. 2008
 20. Lewis RW, Brooks N, Milburn GM, Soames A, Stone S, Hall M, et al. The effects of the phytoestrogen genistein on the postnatal development of the rat. *Toxicol Sci*. 2003; 71:74–83. [PubMed: 12520077]
 21. Jefferson WN, Padilla-Banks E, Newbold RR. Disruption of the female reproductive system by the phytoestrogen genistein. *Reprod Toxicol*. 2007; 23:308–16. [PubMed: 17250991]
 22. Whitten PL, Patisaul HB. Cross-species and interassay comparisons of phytoestrogen action. *Environmental Health Perspectives*. 2001; 109:5–23. [PubMed: 11250801]
 23. Jefferson WN, Padilla-Banks E, Newbold RR. Disruption of the female reproductive system by the phytoestrogen genistein. *Reproductive toxicology (Elmsford, NY)*. 2007; 23:308–16.
 24. Castle EP, Thrasher JB. The role of soy phytoestrogens in prostate cancer. *The Urologic clinics of North America*. 2002; 29:71–81. viii–ix. [PubMed: 12109358]
 25. Dixon RA, Ferreira D. Genistein. *Phytochemistry*. 2002; 60:205–11. [PubMed: 12031439]
 26. Adlercreutz H. Phytoestrogens: epidemiology and a possible role in cancer protection. *Environmental Health Perspectives*. 1995; 130:103–12. [PubMed: 8593855]
 27. Patisaul HB, Jefferson W. The pros and cons of phytoestrogens. *Front Neuroendocrinol*. 2010

28. Setchell KDR, Zimmer-Nechemias L, Cai J, Heubi JE. Exposure of infants to phyto-oestrogens from soy-based infant formula. *Lancet*. 1997; 350:23–7. [PubMed: 9217716]
29. Setchell KD, Zimmer-Nechemias L, Cai J, Heubi JE. Isoflavone content of infant formulas and the metabolic fate of these phytoestrogens in early life. *American Journal of Clinical Nutrition*. 1998; 68:1453S. [PubMed: 9848516]
30. Todaka E, Sakurai K, Fukata H, Miyagawa H, Uzuki M, Omori M, et al. Fetal exposure to phytoestrogens--the difference in phytoestrogen status between mother and fetus. *Environmental research*. 2005; 99:195–203. [PubMed: 16194669]
31. Doerge DR, Twaddle NC, Banks EP, Jefferson WN, Newbold RR. Pharmacokinetic analysis in serum of genistein administered subcutaneously to neonatal mice. *Cancer Lett*. 2002; 184:21–7. [PubMed: 12104044]
32. Jefferson WN, Doerge D, Padilla-Banks E, Woodling KA, Kissling GE, Newbold R. Oral exposure to genistin, the glycosylated form of genistein, during neonatal life adversely affects the female reproductive system. *Environ Health Perspect*. 2009; 117:1883–9. [PubMed: 20049207]
33. Jefferson WN, Couse JF, Padilla-Banks E, Korach KS, Newbold RR. Neonatal exposure to genistein induces estrogen receptor (ER)alpha expression and multiocyte follicles in the maturing mouse ovary: evidence for ERbeta-mediated and nonestrogenic actions. *Biol Reprod*. 2002; 67:1285–96. [PubMed: 12297547]
34. Castellano JM, Gaytan M, Roa J, Vigo E, Navarro VM, Bellido C, et al. Expression of KiSS-1 in rat ovary: putative local regulator of ovulation? *Endocrinology*. 2006; 147:4852–62. [PubMed: 16825322]
35. Gaytan F, Gaytan M, Castellano JM, Romero M, Roa J, Aparicio B, et al. KiSS-1 in the mammalian ovary: distribution of kisspeptin in human and marmoset and alterations in KiSS-1 mRNA levels in a rat model of ovulatory dysfunction. *Am J Physiol Endocrinol Metab*. 2009; 296:E520–31. [PubMed: 19141682]
36. Patisaul HB, Whitten PL, Young L. Regulation of estrogen receptor beta mRNA in the brain: opposite effects of 17 β -estradiol and the phytoestrogen, coumestrol. *Brain Research Molecular Brain Research*. 1999; 67:165–71. [PubMed: 10101243]
37. Hays LE, Carpenter CD, Petersen SL. Evidence that GABAergic neurons in the preoptic area of the rat brain are targets of 2,3,7,8-tetrachlorodibenzo-p-dioxin during development. *Environ Health Perspect*. 2002; 110 (Suppl 3):369–76. [PubMed: 12060831]
38. Cunningham MJ, Scarlett JM, Steiner RA. Cloning and distribution of galanin-like peptide mRNA in the hypothalamus and pituitary of the macaque. *Endocrinology*. 2002; 143:755–63. [PubMed: 11861493]
39. Kuhar MJ, De Souza EB, Unnerstall JR. Neurotransmitter receptor mapping by autoradiography and other methods. *Annu Rev Neurosci*. 1986; 9:27–59. [PubMed: 2423006]
40. Patisaul HB, Scordalakes EM, Young LJ, Rissman EF. Oxytocin, but not oxytocin receptor, is regulated by oestrogen receptor beta in the female mouse hypothalamus. *J Neuroendocrinol*. 2003; 15:787–93. [PubMed: 12834440]
41. Hoffman GE, Le WW. Just cool it! Cryoprotectant anti-freeze in immunocytochemistry and in situ hybridization. *Peptides*. 2004; 25:425–31. [PubMed: 15134865]
42. Franceschini I, Lomet D, Cateau M, Delsol G, Tillet Y, Caraty A. Kisspeptin immunoreactive cells of the ovine preoptic area and arcuate nucleus co-express estrogen receptor alpha. *Neurosci Lett*. 2006; 401:225–30. [PubMed: 16621281]
43. Paxinos, G.; Watson, C. *The rat brain in stereotaxic coordinates*. 6. London: Academic Press; 2007.
44. Smith JT, Dungan HM, Stoll EA, Gottsch ML, Braun RE, Eacker SM, et al. Differential regulation of KiSS-1 mRNA expression by sex steroids in the brain of the male mouse. *Endocrinology*. 2005; 146:2976–84. [PubMed: 15831567]
45. Smith JT, Cunningham MJ, Rissman EF, Clifton DK, Steiner RA. Regulation of Kiss1 gene expression in the brain of the female mouse. *Endocrinology*. 2005; 146:3686–92. [PubMed: 15919741]

46. Ohkura S, Uenoyama Y, Yamada S, Homma T, Takase K, Inoue N, et al. Physiological role of metastin/kisspeptin in regulating gonadotropin-releasing hormone (GnRH) secretion in female rats. *Peptides*. 2009; 30:49–56. [PubMed: 18775461]
47. Adachi S, Yamada S, Takatsu Y, Matsui H, Kinoshita M, Takase K, et al. Involvement of anteroventral periventricular metastin/kisspeptin neurons in estrogen positive feedback action on luteinizing hormone release in female rats. *J Reprod Dev*. 2007; 53:367–78. [PubMed: 17213691]
48. Kuiper GGJM, Lemmen JG, Carlsson B, Corton JC, Safe SH, Van Der Saag PT, et al. Interaction of estrogenic chemicals and phytoestrogens with estrogen receptor β . *Endocrinology*. 1998; 139:4252–63. [PubMed: 9751507]
49. Mueller SO, Kling M, Arifin Firzani P, Mecky A, Duranti E, Shields-Botella J, et al. Activation of estrogen receptor alpha and ERbeta by 4-methylbenzylidene-camphor in human and rat cells: comparison with phyto- and xenoestrogens. *Toxicol Lett*. 2003; 142:89–101. [PubMed: 12765243]
50. Akiyama T, Ishida J, Nakagawa S, Ogawara H, Watanabe S, Itoh N, et al. Genistein, a specific inhibitor of tyrosine-specific protein kinases. *J Biol Chem*. 1987; 262:5592–5. [PubMed: 3106339]
51. Mizukami Y. In vivo functions of GPR30/GPER-1, a membrane receptor for estrogen: from discovery to functions in vivo. *Endocr J*. 2010; 57:101–7. [PubMed: 19996532]
52. Maggiolini M, Picard D. The unfolding stories of GPR30, a new membrane-bound estrogen receptor. *J Endocrinol*. 2010; 204:105–14. [PubMed: 19767412]
53. Filardo EJ, Thomas P. GPR30: a seven-transmembrane-spanning estrogen receptor that triggers EGF release. *Trends Endocrinol Metab*. 2005; 16:362–7. [PubMed: 16125968]
54. Jefferson W, Newbold R, Padilla-Banks E, Pepling M. Neonatal genistein treatment alters ovarian differentiation in the mouse: inhibition of oocyte nest breakdown and increased oocyte survival. *Biol Reprod*. 2006; 74:161–8. [PubMed: 16192398]
55. Chen Y, Jefferson WN, Newbold RR, Padilla-Banks E, Pepling ME. Estradiol, progesterone, and genistein inhibit oocyte nest breakdown and primordial follicle assembly in the neonatal mouse ovary in vitro and in vivo. *Endocrinology*. 2007; 148:3580–90. [PubMed: 17446182]
56. Cimafranca MA, Davila J, Ekman GC, Andrews RN, Neese SL, Peretz J, et al. Acute and chronic effects of oral genistein administration in neonatal mice. *Biol Reprod*. 2010; 83:114–21. [PubMed: 20357267]
57. Reiter EO, Goldenberg RL, Vaitukaitis JL, Ross GT. A role for endogenous estrogen in normal ovarian development in the neonatal rat. *Endocrinology*. 1972; 91:1537–9. [PubMed: 5086150]
58. Pepling ME, Spradling AC. Mouse ovarian germ cell cysts undergo programmed breakdown to form primordial follicles. *Dev Biol*. 2001; 234:339–51. [PubMed: 11397004]
59. Jefferson W, Newbold R, Padilla-Banks E, Pepling M. Neonatal genistein treatment alters ovarian differentiation in the mouse: inhibition of oocyte nest breakdown and increased oocyte survival. *Biology of reproduction*. 2006; 74:161–8. [PubMed: 16192398]
60. Kezele P, Skinner MK. Regulation of ovarian primordial follicle assembly and development by estrogen and progesterone: endocrine model of follicle assembly. *Endocrinology*. 2003; 144:3329–37. [PubMed: 12865310]
61. Bateman HL, Patisaul HB. Disrupted female reproductive physiology following neonatal exposure to phytoestrogens or estrogen specific ligands is associated with decreased GnRH activation and kisspeptin fiber density in the hypothalamus. *Neurotoxicology*. 2008; 29:988–97. [PubMed: 18656497]
62. Jefferson WN, Padilla-Banks E, Newbold RR. Adverse effects on female development and reproduction in CD-1 mice following neonatal exposure to the phytoestrogen genistein at environmentally relevant doses. *Biol Reprod*. 2005; 73:798–806. [PubMed: 15930323]
63. Padilla-Banks E, Jefferson WN, Newbold RR. Neonatal exposure to the phytoestrogen genistein alters mammary gland growth and developmental programming of hormone receptor levels. *Endocrinology*. 2006; 147:4871–82. [PubMed: 16857750]
64. Goldman JM, Laws SC, Balchak SK, Cooper RL, Kavlock RJ. Endocrine-disrupting chemicals: prepubertal exposures and effects on sexual maturation and thyroid activity in the female rat. A focus on the EDSTAC recommendations. *Crit Rev Toxicol*. 2000; 30:135–96. [PubMed: 10759430]

65. Becker JB, Arnold AP, Berkley KJ, Blaustein JD, Eckel LA, Hampson E, et al. Strategies and methods for research on sex differences in brain and behavior. *Endocrinology*. 2005; 146:1650–73. [PubMed: 15618360]
66. Ryan BC, Hotchkiss AK, Crofton KM, Gray LE Jr. In utero and lactational exposure to bisphenol A, in contrast to ethinyl estradiol, does not alter sexually dimorphic behavior, puberty, fertility, and anatomy of female LE rats. *Toxicol Sci*. 2010; 114:133–48. [PubMed: 19864446]
67. Delclos KB, Weis CC, Bucci TJ, Olson G, Mellick P, Sadovova N, et al. Overlapping but distinct effects of genistein and ethinyl estradiol (EE(2)) in female Sprague-Dawley rats in multigenerational reproductive and chronic toxicity studies. *Reprod Toxicol*. 2009; 27:117–32. [PubMed: 19159674]
68. Guerrero-Bosagna CM, Sabat P, Valdovinos FS, Valladares LE, Clark SJ. Epigenetic and phenotypic changes result from a continuous pre and post natal dietary exposure to phytoestrogens in an experimental population of mice. *BMC Physiol*. 2008; 8:17. [PubMed: 18793434]
69. Thigpen JE, Setchell KD, Padilla-Banks E, Haseman JK, Saunders HE, Caviness GF, et al. Variations in phytoestrogen content between different mill dates of the same diet produces significant differences in the time of vaginal opening in CD-1 mice and F344 rats but not in CD Sprague-Dawley rats. *Environ Health Perspect*. 2007; 115:1717–26. [PubMed: 18087589]
70. Thigpen JE, Haseman JK, Saunders HE, Setchell KD, Grant MG, Forsythe DB. Dietary phytoestrogens accelerate the time of vaginal opening in immature CD-1 mice. *Comp Med*. 2003; 53:607–15. [PubMed: 14727808]
71. Roa J, Vigo E, Garcia-Galiano D, Castellano JM, Navarro VM, Pineda R, et al. Desensitization of gonadotropin responses to kisspeptin in the female rat: analyses of LH and FSH secretion at different developmental and metabolic states. *Am J Physiol Endocrinol Metab*. 2008; 294:E1088–96. [PubMed: 18413669]
72. Heindel JJ. The fetal basis of adult disease: Role of environmental exposures--introduction. *Birth Defects Res A Clin Mol Teratol*. 2005; 73:131–2. [PubMed: 15751038]
73. Barker DJ. Maternal nutrition, fetal nutrition, and disease in later life. *Nutrition*. 1997; 13:807–13. [PubMed: 9290095]
74. Aksglaede L, Sorensen K, Petersen JH, Skakkebaek NE, Juul A. Recent decline in age at breast development: the Copenhagen Puberty Study. *Pediatrics*. 2009; 123:e932–9. [PubMed: 19403485]
75. Biro FM, Galvez MP, Greenspan LC, Succop PA, Vangeepuram N, Pinney SM, et al. Pubertal Assessment Method and Baseline Characteristics in a Mixed Longitudinal Study of Girls. *Pediatrics*. 2010
76. Crain DA, Janssen SJ, Edwards TM, Heindel J, Ho SM, Hunt P, et al. Female reproductive disorders: the roles of endocrine-disrupting compounds and developmental timing. *Fertil Steril*. 2008; 90:911–40. [PubMed: 18929049]

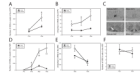


Fig. 1.

The ontogeny of KISS neuronal development is sex specific in both the AVPV and the ARC and is reliably captured by quantifying the density of fibers immunoreactive for KISS in each region. (A) The density of KISS-ir fibers increases across peripubertal development in both sexes with females having twice as many as males by P30. (B) Ontogeny of AVPV Kiss1 mRNA is similar with expression levels three times that of males by P30. (C) Representative autoradiographs depicting Kiss1 mRNA expression in P30 males in females in the AVPV (upper panels) and ARC (lower panels). (D) In the ARC, the density of KISS-ir fibers rapidly increases in females between P10 and 20 while male levels remain relatively flat between P5 and P30. (E) This sex difference in fiber density is not recapitulated in mRNA levels which instead only show a trend for a sex difference on P20. (F) Immunopositive cell bodies in the ARC are difficult to discern from dense fiber labeling but the number of KISS neurons does not appear to be sex specific. (mean \pm SEM; ‡ $p \leq 0.1$, * $p \leq 0.05$, ** $p \leq 0.01$)

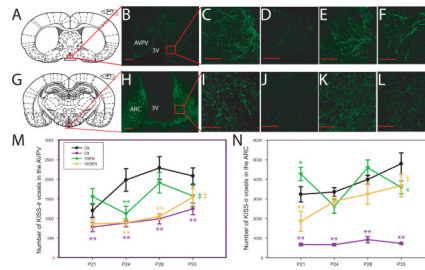


Fig. 2.

Diagrammatic (A and G) and representative confocal images (single image planes) depicting KISS-ir labeling in the AVPV (B-F) and ARC (H-L). Labeling was readily observed within extended lengths of fibers in both regions (10x for B and H, 40x for all others). (C-F) KISS-ir in the AVPV of control (OIL), EB, 1GEN and 10GEN exposed animals respectively, all collected on P28. Labeling was highest in the OIL animals and lowest in the EB animals. (I-L) KISS-ir in the ARC of P28 OIL, EB, 1GEN and 10GEN exposed animals respectively. (M) AVPV KISS-ir fiber density was significantly lower in the EB and 10GEN exposed animals compared to OIL controls at all ages examined. Levels in 1GEN females were generally found to be in between OIL and EB females (N) KISS-ir fiber density in the ARC was significantly lower in the EB exposed animals at all time points. Levels generally lower in 10GEN animals but this difference was only statistically significant on P21. Levels in 1GEN animals oscillated around OIL levels and were therefore more difficult to interpret (mean \pm SEM; scalebar = 50 μ m ‡ $p \leq 0.1$, * $p \leq 0.05$, ** $p \leq 0.01$)

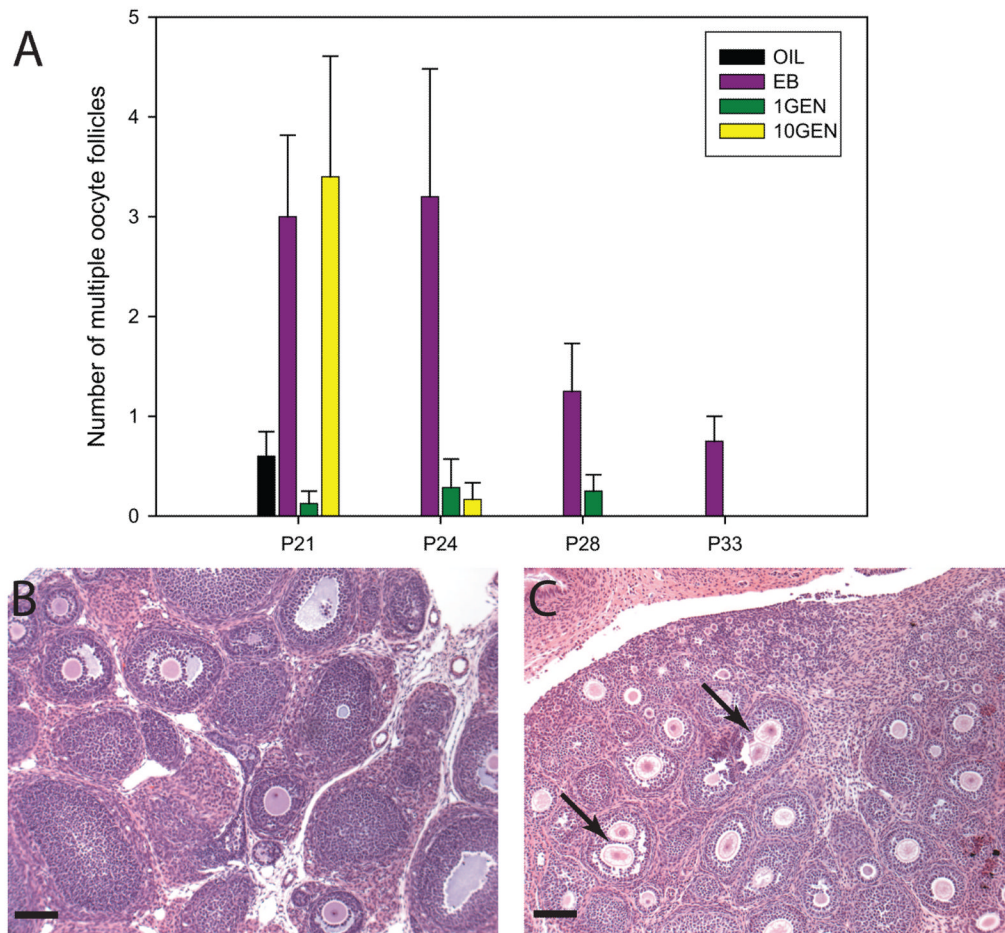


Fig. 3.

(A) The average number of multiple oocyte follicles (MOFs) found in the different exposure groups at each age, with control (OIL) animals having no MOFs by P24, EB exposed animals having MOFs at all time points and 10GEN exposed animals having MOFs through P24. Because of technical issues, tissue from P28 and P33 10GEN females, and P33 OIL animals was not available. Representative images (taken at 20x) depicting ovarian follicles from P21 OIL (B) and 10GEN (C) females. MOFs (arrows) were readily apparent in the 10GEN ovary. (scalebar = 40 μ m)

Table 1

Table showing the number of animals in each exposure group (N), the number of dams these animals were obtained from, as well as the number of animals displaying vaginal opening on the day of perfusion. EB exposed animals underwent vaginal opening first, followed by the 10GEN exposed animals, the 1GEN exposed animals and finally the control animals (OIL).

	P21			P24			P28			P33		
	N	# Dams	Vaginal opening	N	# Dams	Vaginal Opening	N	# Dams	Vaginal Opening	N	# Dams	Vaginal Opening
OIL	8	3	0 of 8	7	5	0 of 7	8	4	0 of 8	7	6	7 of 7
EB	8	5	2 of 8	7	4	7 of 7	7	4	7 of 7	7	4	7 of 7
1GEN	7	3	0 of 7	8	3	0 of 7	8	3	8 of 8	9	4	9 of 9
10GEN	7	3	0 of 7	7	3	0 of 7	6	3	6 of 6	7	5	7 of 7